Bull. Chem. Soc. Jpn., 55, 2046—2050 (1982) [Vol. 55, No. 7

Optical Studies on the Lowest Triplet State of Chromone

Yasuko Yamada, Seigo Yamauchi,* and Noboru Hirota*
Department of Chemistry, Faculty of Science, Kyoto University,
Kitashirakawaoiwake-cho, Sakyo-ku, Kyoto 606
(Received January 18, 1982)

The lowest excited triplet state of chromone was investigated *via* high resolution phosphorescence spectra, phosphorescence excitation spectra and triplet lifetimes in the neat crystal, in the single crystals of durene and benzoic acid at liquid helium temperature. Including the cases in other solvents such as 3-methylpentane, methylcyclohexane and ethanol, the lowest triplet state was assigned to be $\pi\pi^*$ type contrary to the previous assignment. The triplet sublevel properties including the sublevel spectra were obtained in the benzoic acid host. T_y is radiative at the 0-0 band. T_z is radiative at the nontotally symmetric bands and is active in nonradiative transitions. These properties are discussed and compared with those of other carbonyl compounds. A brief comment on the photochemical reactions are given.

There have been some interests in the photochemical behavior of chromone (**1**) and several works have been reported in recent years.1—4) It has been suggested that the lowest excited triplet state T_1 is involved in the photochemical reactions and the orbital character ($n\pi^*$ or $\pi\pi^*$) of the T_1 state has been discussed from the photoproducts. $n\pi^*$ assignment was favored in these works.

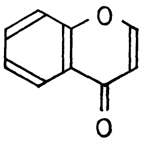
1

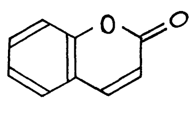
2

The phosphorescence spectra and triplet lifetimes at 77 K have been reported by Hanifin and Cohen,1) Gallivan,5) and Brinen.6) They assigned the lowest triplet state to be $\pi\pi^*$ type in ethanol, but $n\pi^*$ in 3-methylpentane and 2-methyltetrahydrofuran based on the spectra and the lifetimes of 15—38 ms. This assignment, however, is questionable for the following reasons. Firstly, the reported phosphorescence spectra are too complex to be assigned to $n\pi^*$ spectra.7) Secondly, the lifetimes of 15—38 ms appear to be somewhat long as lifetimes of $^3n\pi^*$ states. Furthermore, the use of lifetimes as a criterion to decide the triplet character is sometimes ambiguous, because the lifetimes of the $\pi\pi^*$ carbonyls at 77 K may be markedly shortened by thermal mixing with higher vibronic states and second triplet ($^3n\pi^*$) states.7)

In order to decide the character of the T_1 state unambiguously, we have taken high resolution phosphorescence emission and excitation spectra and measured the lifetimes in different host crystals at liquid helium temperature. Comparing the obtained spectra with those of typical $^3n\pi^*$ and $^3\pi\pi^*$ types, we discuss whether the T_1 state is $^3n\pi^*$ or $^3\pi\pi^*$ in nature. The lifetimes and excitation spectra are used to confirm the assignment. We also discuss a correlation between the phosphorescence properties and ΔE_{TT} (energy difference between T_1 and T_2).

In a previous work we have studied the properties of the T_1 state of coumarin (**2**) which is isomeric to chromone.8) It was found that the decay properties of coumarin are very different from those of benzaldehyde type aromatic carbonyls. This difference was thought to arise from the large difference in ΔE_{TT}. It seemed interesting to examine the decay properties of chromone in this connection. Accordingly, we have made zero field optically detected magnetic resonance (ODMR) experiments in benzoic acid host to obtain the zero field splitting, the total decay rate constants from sublevels, the relative decay rate constants and sublevel spectra. We discuss the mechanisms of the radiative and non-radiative transitions and compare the properties with those of other carbonyls. Lastly we briefly comment on the implication of the present work on the photochemical behavior of chromone.

Experimental

Chromone, durene, and benzoic acid were purified by zone melting after recrystallization from ethanol. Single crystals were grown by the Bridgman method. The mole fractions of chromone were *ca.* 10^{-2} in the melts, but those of the samples used in the experiments were not measured.

The phosphorescence emission and excitation spectra were obtained at 4.2 K with an Osram 900 W Xe lamp, a Spex 1704 1 m monochromator and an EMI 9502 photomultiplier. The excitation spectra were observed by monitoring the total phosphorescence. The phosphorescence lifetimes were obtained at 1.4 K. The zero field ODMR and microwave induced delayed phosphorescence (MIDP) experiments were made using the mixed crystal of benzoic acid with the apparatus already described.9) The individual triplet spin sublevel spectra were obtained by observing the time resolved spectra and MIDP spectra at 1160 ms after excitation cut-off, with a PAR 160 boxcar integrator.10)

Results

The phosphorescence spectra of chromone obtained at 4.2 K in the neat crystal, in the single crystals of durene and of benzoic acid are shown in Fig. 1. The 0-0 band was observed at 379.29 nm, 383.08 nm, and 382.91 nm, respectively. Three sites were observed in benzoic acid as shown in the figure. The triplet lifetimes at 1.4 K are shown in Table 1. In the case of benzoic acid, the lifetime of site III is tabulated. Even at 1.4 K chromone in benzoic acid shows a single exponential decay except in the site I. The lifetime in the durene host at 77 K is 8 ms, which is markedly shorter than that at 1.4 K.

$\Delta E_{TT}(=E(T_2)-E(T_1))$ obtained from the phospho-

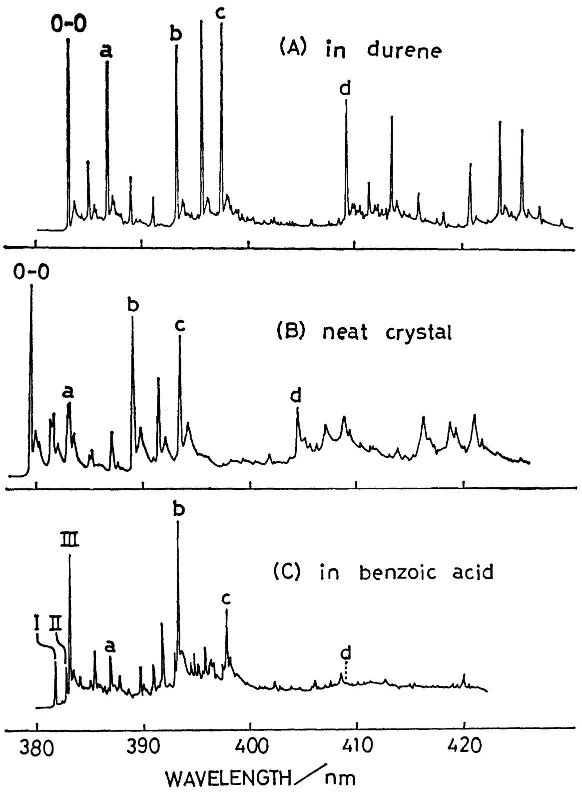

Fig. 1. Phosphorescence spectra of chromone at 4.2 K in durene(A), in a near crystal (B), and in benzoic acid(C).
I, II, and III denote the 0-0 bands of the three sites. a, b, c, and d represent 0-252 cm^{-1}, 0-682 cm^{-1}, 0-980 cm^{-1} bands (see Table 3.) and C=O stretching band respectively.

Table 1. Phosphorescence lifetimes and energy gaps between $T_1(\pi\pi^*)$ and $T_2(n\pi^*)$ states of chromone

Host	Lifetime/ms	ΔE_{TT}/cm^{-1}
Durene	35	371
Neat	55	539
Benzoic acid	241	2356

rescence excitation spectra are also shown in Table 1. A typical excitation spectrum in a lower energy region is shown in Fig. 2. The 0-0 bands of the T_1 and T_2 states are assigned as shown in the figure. In the benzoic acid host, the $S_0 \rightarrow T_2$ ($n\pi^*$) absorption is buried under the $S_0 \rightarrow T_1$ absorption of the benzoic acid. In order to estimate an approximate value we used $\Delta E'_{ST}=1750$ cm^{-1} ($\Delta E'_{ST}=E(^1n\pi^*)-E(^3n\pi^*)$), obtained from the neat crystal. This value is known to be appropriate in a series of substituted benzaldehydes.[11]

Spin sublevel properties could be investigated only for the site I in benzoic acid, where the spin-lattice relaxation was suppressed. The zero field splitting constants, the total decay rate constants and the relative radiative decay rate constants at vibronic bands are given in Table 2. The T_z and T_y sublevel spectra are shown in Fig. 3.

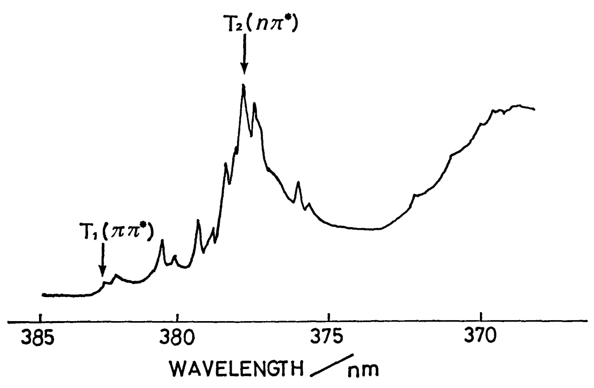

Fig. 2. Phosphorescence excitation spectrum of chromone in durene at 4.2 K.
The 0-0 bands of $T_1(\pi\pi^*)$ and $T_2(n\pi^*)$ are shown.

Table 2. Sublevel energies, total deday rate constants, and relative radiative decay rate constants of the lowest triplet state of chromone in benzoic acid

	$\varepsilon_i^{a)}$/GHz	k_i/s^{-1}	k_i^r(rel)	
			0-0	0-682 cm^{-1}
T_z	1.29	6.79	0.24	1.00
T_y	0.82	2.19	1.00	0.12
T_x	−2.11	0.21	0.11	0.03

a) $\varepsilon_z+\varepsilon_y+\varepsilon_x=0$.

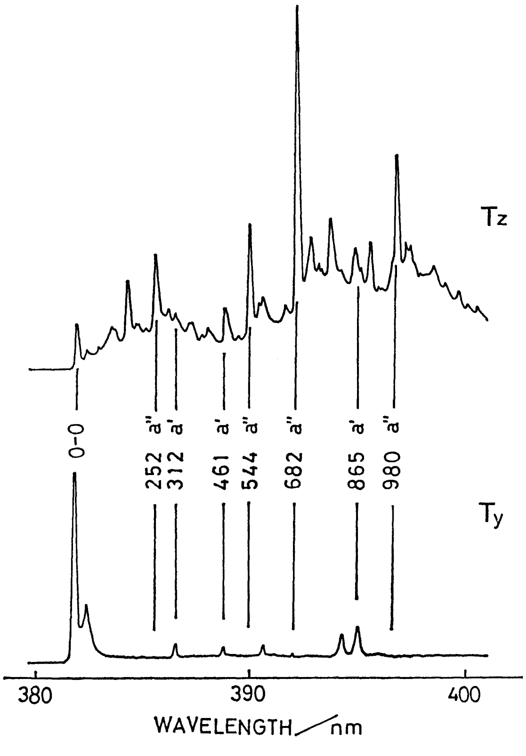

Fig. 3. T_z and T_y sublevel phosphorescence spectra of chromone in benzoic acid.
Vibrational analysis is summarized in Table 3.

Discussion

Assignment of the Lowest Triplet State. In many aromatic carbonyl compounds, phosphorescence spectra are quite different, depending on whether the lowest triplet states are nπ^* or $\pi\pi^*$ type.[7,12,13] If a phosphorescence state is of nπ^* character, its spectrum is very simple consisting mainly of a 0-0 band and vibronic bands involving C=O stretching vibration. Occasionally bands involving nontotally symmetric vibrations give rise to strong progressions due to molecular distortion.[14,15] On the other hand, a $\pi\pi^*$ triplet state gives a more complicated spectrum because of a nπ^*—$\pi\pi^*$ vibronic coupling. Especially when a ^{3}nπ^* triplet state is located near a $^3\pi\pi^*$ state, a spectrum is composed of many vibronic bands of comparable intensities.[13]

Keeping these facts in mind, we examine the spectra in Fig. 1. In all spectra, many strong bands appear in addition to the 0-0 band and the C=O stretching band. Any progression except the C=O stretching band is not observed. Obviously these are the characteristics of the $^3\pi\pi^*$ phosphorescence spectra. Almost all the strong bands in these spectra except the C=O band must be the bands involving nontotally symmetric vibrations. Detailed vibrational assignment is given in the later section.

The phosphorescence excitation spectra support this conclusion. The intensity of the 0-0 band of T_1 is much weaker than the vibronic bands and the 0-0 band of T_2 (Fig. 2). The phosphorescence lifetimes of 35—241 ms are also consistent with the $\pi\pi^*$ assignment. The lifetime of a ^{3}nπ^* carbonyl is usually in the order of at most a few milliseconds.[12] Combined with all of these facts, the lowest triplet states of chromone in these hosts are definitely assigned to be of $\pi\pi^*$ character. Judging from the lifetimes and spectra, the T_1 states in 3-methylpentane and 2-methyltetrahydrofuran previously assigned to be nπ^* states are also assigned to be of the $\pi\pi^*$ type, though ΔE_{TT} is relatively small. In all other solvents we examined, hexane, methylcyclohexane, and ethanol, T_1 was found to be of $\pi\pi^*$ type.

Next we discuss a correlation between ΔE_{TT} and some properties of phosphorescence. ΔE_{TT} increases in the order, in durene, in neat crystal, in benzoic acid. The total decay rate constant and the relative intensity of the C=O band decrease in the same order. This correlation is interpreted in terms of a magnitude of the mixing between $T_1(\pi\pi^*)$ and T_2(nπ^*) states, that is, how much ^{3}nπ^* state character is contaminated in T_1 state determines the properties of T_1 in durene and neat crystal.

Radiative and Non-radiative Mechanisms for the Triplet Spin Sublevels. With the MIDP technique, the relative radiative decay rate constants of the vibronic bands are obtained as $k_z^r(0\text{-}0):k_y^r(0\text{-}0):k_x^r(0\text{-}0)=0.24:1:0.11$ and $k_z^r(0\text{-}682\ \mathrm{cm}^{-1}):k_y^r(0\text{-}682\ \mathrm{cm}^{-1}):k_x^r(0\text{-}682\ \mathrm{cm}^{-1})=1:0.12:0.03$. Together with these values, the spin sublevel spectra (Fig. 3) give the ratio of the total radiative decay rate constants as $k_y^r \gtrsim 0.3k_z^r$ $(k_i^r \equiv \sum_{\nu} k_i^r(\nu))$. If we use the equation $k_y \simeq 0.3k_z$ (Table 2) and the inequality $k_y^r \gtrsim 0.3k_z^r$, we can obtain $k_y^{nr} \lesssim 0.3k_z^{nr}$. The spin sublevel spectra also show that the ratio of the radiative decay at the nontotally symmetric bands of strong intensities are nearly equal to that of the 0-682 cm^{-1} band. Therefore, T_y is radiative at the 0-0 band, whereas T_z is radiative at the nontotally symmetric bands and also active in the nonradiative transition. T_x is less active in both radiative and nonradiative transitions. The symmetry of the molecule is C_s and the lowest triplet state belongs to A$'(\pi\pi^*)$. If we assume that one center integral at the oxygen atom is dominant in the relevant spin orbit coupling matrix elements, the T_z and T_y sublevels couple with the ^{1}nπ^* and $^1\sigma\pi^*$ states, respectively.

Radiative Mechanisms: The radiative mechanisms at the 0-0 band and the totally symmetric a$'$ bands are summarized as follows,

$$T_z \xrightarrow{H_{so}(1)} {}^1\mathrm{n}\pi^*(A'') \xrightarrow{er} S_0, \tag{1}$$

$$T_y \xrightarrow{H_{so}(1)} {}^1\sigma\pi^*(A'') \xrightarrow{er} S_0, \tag{2}$$

$$\xrightarrow{H_{so}(2)} {}^1\mathrm{n}\pi^*(A'') \xrightarrow{er} S_0, \tag{3}$$

$$T_x \xrightarrow{H_{so}(3)} {}^1\pi\pi^*(A') \xrightarrow{er} S_0. \tag{4}$$

H_{so} and e$\boldsymbol{r}$ denote a spin orbit coupling and a dipole transition, respectively. H_{so} (1), H_{so} (2), and H_{so} (3) represent matrix elements which involve one center, two center and three center atomic integrals. $\sigma\pi^*$ denotes botn $\sigma\pi^*$ and $\pi\sigma^*$ states. The contribution of the two center terms involving the $\sigma\pi^*$ states is neglected because of the weak coupling due to the large energy denominator. The magnitude of the spin orbit coupling is large in both T_z and T_y owing to one center terms. Although the energy denominator $(\Delta E_{ST}=E(S)-E(T_1))$ is favorable for T_z, the transition dipole moment for the $S_0 \rightarrow S_1$ (nπ^*) transition is expected to be much smaller than those for the $S_0 \rightarrow S_i$ ($\sigma\pi^*$) transitions. Indeed, CNDO/S calculation on chromone predicts that the oscillator strengths for the $S_0 \rightarrow S_i$ ($\sigma\pi^*$) transitions are about two orders of magnitude larger than that for the $S_0 \rightarrow S_1$ (nπ^*) transition. Considering these factors, we expect that T_y is more radiative than T_z at the 0-0 and a$'$ bands. T_x will be only slightly active owing to three center terms. These expectations are born out by the observation, $k_z^r(0\text{-}0):k_y^r(0\text{-}0):r_x^r(0\text{-}0)=0.24:1:0.10$. As a result the mechanism (2) is the most important in the radiative decay at the 0-0 band.

For the nontotally symmetric bands, we must consider vibronic couplings. We will discuss the mechanisms paying attention to the result, $k_z^r(\mathrm{nt}):k_y^r(\mathrm{nt})=1:0.12$ (nt denotes to nontotally symmetric vibronic bands.). The mechanisms similar to the mechanisms (1)—(4) are summarized as follows:

$$T_z \xrightarrow{a''} {}^3\mathrm{n}\pi^*(A'') \xrightarrow{H_{so}(1)} {}^1\pi\pi^*(A') \xrightarrow{er} S_0, \tag{5}$$

$$\xrightarrow{H_{so}(1)} {}^1\mathrm{n}\pi^*(A'') \xrightarrow{a''} {}^1\pi\pi^*(A') \xrightarrow{er} S_0, \tag{6}$$

$$T_y \xrightarrow{a''} {}^3\sigma\pi^*(A'') \xrightarrow{H_{so}(1)} {}^1\pi\pi^*(A') \xrightarrow{er} S_0, \tag{7}$$

$$\xrightarrow{a''} {}^3\mathrm{n}\pi^*(A'') \xrightarrow{H_{so}(2)} {}^1\pi\pi^*(A') \xrightarrow{er} S_0, \tag{8}$$

$$\xrightarrow{H_{so}(1)} {}^1\sigma\pi^*(A'') \xrightarrow{a''} {}^1\pi\pi^*(A') \xrightarrow{er} S_0, \tag{9}$$

$$\xrightarrow{H_{so}(2)} {}^1n\pi^*(A'') \xrightarrow{a''} {}^1\pi\pi^*(A') \xrightarrow{er} S_0. \tag{10}$$

The difference between T_z and T_y is that T_z involves a spin orbit coupling with the nπ^* state *via* one center terms, while T_y involves spin orbit coupling with the $\sigma\pi^*$ states via one center terms and with the nπ^* state *via* two center terms. As the $\sigma\pi^*$ states are higher in energy and the two center terms are smaller, T_z is expected to be more active at the nontotally symmetric bands. This expectation was again realized by the observation, $k_z^r(\mathrm{nt}):k_y^r(\mathrm{nt})=1:0.12$. Next we discuss the relative importance of $\sigma\pi^*$ and nπ^* states as the intermediate in the T_y mechanism. In the T_y radiative decay at the nontotally symmetric bands, the mechanism involving the $\sigma\pi^*$ states ((7), (9)) is likely to be more important than that involving the nπ^* state, because the magnitude of one center terms is expected to be more than 100 times of that of two center terms as found in the case of quinoxaline.[10] T_x sublevel is again less active because of the three center terms A detailed vibrational assignment is made by the sublevel spectra and fm-ODMR spectra and is shown in Table 3. In-plane (a′) and out-of-plane (a″) vibrations are distinguished.

Nonradiative Mechanisms: The mechanisms of the nonradiative transitions resemble to those of radiative transitions of vibronic bands (*cf.* mechanism (5)—(10)). The mechanisms are the following, based on the foregoing discussion.[16]

$$T_z \xrightarrow{a''} {}^3n\pi^*(A'') \xrightarrow{H_{so}(1)} S_0, \tag{11}$$

$$\xrightarrow{H_{so}(1)} {}^1n\pi^*(A'') \xrightarrow{a''} S_0, \tag{12}$$

$$T_y \xrightarrow{a''} {}^3\sigma\pi^*(A'') \xrightarrow{H_{so}(1)} S_0, \tag{13}$$

$$\xrightarrow{H_{so}(1)} {}^1\sigma\pi^*(A'') \xrightarrow{a''} S_0, \tag{14}$$

$$T_x \xrightarrow{H_{so}(3)} S_0. \tag{15}$$

As in the case of radiative transition at the nontotally symmetric bands, T_z involves the spin orbit coupling with the nπ^* states and T_y with the $\sigma\pi^*$ states, and the energy denominator favors the T_z mechanism. Similar results for $k_z^r(\mathrm{nt})/k_y^r(\mathrm{nt})$ and k_z^{nr}/k_y^{nr} are expected. As expected, T_z is most active in the nonradiative transition. Although T_x involves direct coupling with the ground state, T_x is not expected to be active, again due to three center atomic integrals.

TABLE 3. VIBRATIONAL ANALYSIS OF THE PHOSPHORESCENCE SPECTRUM OF CHROMONE IN BENZOIC ACID

Wavelength/nm	Wave number/cm^{-1}	$\Delta\nu$/cm^{-1}	Assignment
381.62	26197	0	
384.01	26034	163	a″
385.32	25945	252	a″
386.22	25885	312	a′
388.45	25736	461	a′
388.54	25730	467	a″
389.71	25653	544	a″
390.39	25608	589	a′
391.82	25515	682	a″
393.45	25409	788	a″
393.89	25381	816	a′
394.52	25340	857	a″
394.65	25332	865	a′
395.22	25295	902	a″
396.44	25217	980	a″

Comparison with Other Carbonyl Compounds. We compare the dynamical properties of chromone in benzoic acid with those of coumarine (**2**) in durene,[8] anti-(CH$_3$,H)bimane(4,8-dimethyl-1,5-diazabicyclo[3.3.0]octa-3,7-diene-2,6-dione) (**3**) in durene[17] and benzaldehyde (**4**) in benzoic acid.[18]

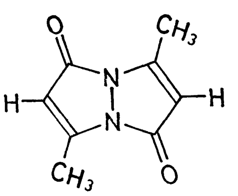

3

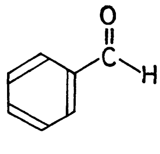

4

In all cases, the lowest triplet states are of $\pi\pi^*$ type with relatively large ΔE_{TT} (2300—6300 cm^{-1}). In coumarin (k_z=9.7 s^{-1}, k_y=2.0 s^{-1}, k_x=0.32 s^{-1}; k_z^r(0-0):k_y^r(0-0):k_x^r(0-0)=0.25:1:0.03) and anti-bimane (k_z=1.83 s^{-1}, k_y=2.99 s^{-1}, k_x=0.14 s^{-1}; k_z^r(0-0):k_y^r(0-0):k_x^r(0-0)=0.04:1:0.02) these properties are very similar to those of chromone, T_y is radiatively active at the 0-0 band, whereas T_z is active in the nontotally symmetric bands. On the other hand in benzaldehyde (k_z=18 s^{-1}, k_y=0.44 s^{-1}, k_x=0.46 s^{-1}; k_z^r(0-0):k_y^r(0-0):k_x^r(0-0)=1:0.06:0.06) and substituted benzaldehydes, k_y is not large and T_y is less radiative even at the 0-0 band. Possible reasons for the difference between the two types of molecules are the following.

(1) The oscillator strength for the $S_0 \rightarrow S_1$ (nπ^*) transition is larger in benzaldehyde type molecules. This has been found experimentally[19] and is also supported by the CNDO/S calculation.

(2) The energies of the $\sigma\pi^*$ states are lower in chromone than in benzaldehyde. The oscillator strengths for the $S_0 \rightarrow S_i$ ($\sigma\pi^*$) transitions for the lower energy states may be larger for chromone and coumarin as indicated by the results of CNDO/S calculation.

Comment on the Photochemical Reactions. We have assigned T_1 of chromone as $\pi\pi^*$ states in all solvents and host crystals at low temperatures. This is somewhat contradictory to the conclusion derived from the photochemical studies. In the non-polar solvents ΔE_{TT} is in the same order of magnitude as measured in the durene crystal (ΔE_{TT}=371 cm^{-1}). With this value of ΔE_{TT} the ratio between the population in the ^{3}nπ^* and that in the T_1 state in Boltzmann distribution is 0.17 at 300 K. Therefore, it is quite probable that both ^{3}nπ^* and $^3\pi\pi^*$ type photochemical reactions take place. Although the phosphorescence spectra and lifetimes indicate the mixed character of the T_1 state, the actual nπ^* character induced by the vibronic mixing is at most 3%. Thus the thermal population of the ^{3}nπ^* state is likely to be responsible for the ^{3}nπ^* type reaction.

The report that the $^3n\pi^*$ type reaction takes place in methanol[3] is puzzling. ΔE_{TT} in methanol is in the same order as that in benzoic acid and the ratio of the population of the $^3n\pi^*$ state is *ca.* 10^{-5} at 300 K. It is possible that chromone in solution at 300 K has a smaller ΔE_{TT} than that estimated in solid at 4.2 K or has a considerably different configuration. However, whether or not a $^3n\pi^*$ type reaction is really taking place still seems to be uncertain.

We wish to thank Dr. Tadamasa Shida for discussions on CNDO/S calculations, and Mr. Masaaki Baba for experiments.

References

1) J. W. Hanifin and E. Cohen, *J. Am. Chem. Soc.*, **91**, 4494 (1969).

2) R. Matsushima, T. Kishimoto, M. Suzuki, M. Morioka, and H. Mizuno, *Bull. Chem. Soc. Jpn.*, **53**, 2938 (1980).

3) Y. Yamamoto and E. Toyota, *Chem. Pharm. Bull.*, **26**, 2277 (1978).

4) K. Hamanoue, T. Nakayama, T. Miyake, and H. Teranishi, *Chem. Lett.*, **1981**, 39.

5) J. B. Gallivan, *Can. J. Chem.*, **48**, 3938 (1970).

6) J. B. Gallivan and J. S. Brinen, *Chem. Phys. Lett.*, **10**, 455 (1971).

7) L. Goodman and M. Koyanagi, *Mol. Photochem.*, **4**, 369 (1972).

8) E. T. Harrigan, A Chakrabarti, and N. Hirota, *J. Am. Chem. Soc.*, **98**, 3460 (1976).

9) T. H. Cheng and N. Hirota, *J. Chem. Phys.*, **56**, 5019 (1972); J. Schmidt, W. S. Veeman, and J. H. van der Waals, *Chem. Phys. Lett.*, **4**, 341 (1969); D. A. Antheunis, J. Schmidt, and J. H. van der Waals, *ibid.*, **6**, 255 (1970); *Mol. Phys.*, **22**, 1 (1971).

10) S. Yamauchi and T. Azumi, *J. Chem. Phys.*, **68**, 4138 (1978).

11) H. Hayashi and S. Nagakura, *Mol. Phys.*, **27**, 969 (1974).

12) E. T. Harrigan and N. Hirota, *Mol. Phys.*, **31**, 681 (1976).

13) A. Després, V. Lejeune, E. Migirdicyan, and W. Siebrand, *Chem. Phys.*, **36**, 41 (1979).

14) S. Yamauchi and D. W. Pratt, *Mol. Phys.*, **37**, 541 (1979).

15) M. Baba and N. Hirota, *Chem. Phys. Lett.*, **64**, 321 (1979).

16) F. Metz, S. Friedrich, and G. Hohlneicher, *Chem. Phys. Lett.*, **16**, 353, (1972).

17) M. Baba, N. Hirota, and E. M. Kosower, *J. Phys. Chem.*, **85**, 1469 (1981).

18) Y. Hirata and N. Hirota, *Mol. Phys.*, **39**, 129 (1980).

19) Y. Kanda, H. Kaseda, and T. Matsumura, *Spectrochim. Acta, Part A*, **20**, 1387 (1964).